Excitation of the NO molecule by chirped infrared laser pulses

J. T. Lin, M. Hayashi, and S. H. Lin
Institute of Atomic and Molecular Sciences, Academia Sinica, Taipei, Taiwan

T. F. Jiang*
Department of Chemistry, University of Kansas, Lawerence, Kansas 66045
(Received 25 November 1998; revised manuscript received 10 June 1999)

To explore the insights of recent experiments on the excitation of the NO molecule by chirped subpicosecond IR pulses, a corresponding theoretical study is presented. The agreements between experimental and theoretical results show the importance of the full-dimensional quantum-mechanical calculation. [S1050-2947(99)04711-3]

PACS number(s): 42.50.Hz, 31.15.Qg, 31.70.Hq

I. INTRODUCTION

The coherent control of molecular photoexcitation has attracted increasing interest recently [1–8]. One facet of which is the excitation of the molecule into a specific highly excited vibrational state in order to enhance the chemical activity. There are several routes to reach this goal, such as stimulated emission pumping (SEP) [9,10] and stimulated rapid adiabatic passage (SRAP) [11], which have successfully prepared highly excited vibrational states in small molecules by using long laser pulses. Although these methods can excite the molecules to highly excited vibrational states, there are still some problems to overcome. For example, the transition dipole moment between the initial and final states is small and hence the few-photon absorption processes are inefficient; increasing the pulse intensity certainly may enhance the excitation probability, but other side effects, such as the deformation of potential-energy surfaces and the ionization processes, will occur. Besides, the characteristic time of the laser pulse is longer than the time scale of the intramolecular vibrational relaxation (IVR) processes so that the bond-selective excitation becomes impossible [12,13].

As proposed by Chelkowski and Bandrauk [3], an optimal stepwise chirped pulse is able to provide a solution for overcoming the anharmonicity of the molecular potential, and reducing the pulse intensity for significant population. They derived the optimal chirped pulses by using the π-pulse criterion of a two-level system [14]. Unfortunately this kind of pulse is very hard to construct experimentally. Actually the ladder-climbing processes are far more complicated than the two-level ''π-pulse'' criterion if the rotational states are taken into consideration. Liu and co-workers [7,8] and our previous works [15,16] have shown that linear chirped pulses almost have the same efficiency as Chelkowski and Bandrauk's optimal pulses, both in quantum and classical calculations. However, when the chirping is performed, a weaker condition on the chirping rate is needed: $|d\omega(t)/dt| \ll \Omega_{Rabi}^2(t)$. That is, the chirping rate should be sufficiently slow, compared to the Rabi frequency $\Omega_{Rabi}(t)$, in order to transfer the population in the adiabatic regime.

Recently, Maas and co-workers performed the *first* experiment of NO molecular excitation by a *linear* chirped free-electron laser [17,18]. They showed the robustness of such a type of linear chirped pulse (called FELIX, the free-electron laser for infrared experiments) excitation against the instability of pulse characteristics. They found that the third vibrational excited state can be reached with FELIX. Moreover, the correct and incorrect directions of chirping cause an eight times difference in the excitation populations; and they also showed the possibility of applying such an ultrashort pulse to pump laser energy into the selected bond and localizing in the specific state for the polyatomic molecules within 1 ps. We will address in this paper the theoretical study of the corresponding experiment. A detailed full-dimensional quantum simulation will prove to reproduce the experimental data well.

In most situations, the one-dimensional (1D) model for a diatomic molecule is frequently employed to examine the molecular behavior under the interaction with a light field. However, a majority of these studies have neglected the rotational effect and the coupling between rotational and vibrational states. The 1D model also assumes that the molecular axis is perfectly aligned along the external field axis throughout the interaction time, and is much easier to calculate than the full-dimensional study [1,16,19,20]. Our previous studies [16] show that, although the chirping excitation dynamics are roughly similar to each other for the 1D and full-dimensional cases, the field duration must be longer and field intensity must be stronger for the real molecule to have the same populations and dissociation probability as the 1D model. This is because the full-dimensional molecule has a weaker dipole moment than the 1D model. To mimic the realistic field-molecule interaction, we must include the rotational effect in the excitation process.

II. CALCULATION METHOD

The system we study here is the NO molecules irradiated by a chirped IR laser pulse. Under the Born-Oppenheimer approximation, the vibrational and rotational states in the ground electronic state can be described by the solution of the Hamiltonian

*Permanent address: Institute of Physics, National Chiao Tung University, Hsinchu 30050, Taiwan.

$$\hat{H}_0=\frac{-\partial^2}{2\mu\partial R^2}+\frac{\hat{L}^2}{2\mu R^2}+D_e[1-e^{-\beta(R-R_0)}]^2. \quad (1)$$

To model the NO molecule, the potential parameters $D_e=0.2388$ a.u., $\beta=1.4648$ a.u., $\mu=13\,709.9499$ a.u., and $R_0=2.175$ a.u. are used. Here R denotes the relative coordinate of the atomic nuclei and μ represents the reduced mass of atoms N and O [7,8]. Atomic units are used hereafter unless otherwise stated. Omitting the rotational term $\hat{L}^2/2\mu R^2$ reduces the system to the 1D model. In addition, the unperturbed Hamiltonian supports 55 vibrational bound states; rotational levels are associated with each vibrational state as well. The electric field of the chirped pulse can be expressed as

$$\mathbf{E}(t)=E_m\mathbf{e}_z\frac{1}{2}\{\exp(-\Gamma t^2)\exp[i\phi(t)]+\text{c.c.}\}, \quad (2)$$

where $\phi(t)=\int_{-\infty}^{t}\omega(t')dt'$ is the phase of the pulse at time t with chirped frequency $\omega(t)$. The light pulse is chirped by passing through a pulse shaper that is centered around ω_0 with a small bandwidth $\Delta\omega$ and duration τ_0 [18,21]. The output light is then composed of the different phase delay components with a new bandwidth parameter

$$\Gamma=\frac{8\dfrac{\ln 2}{\Delta\omega^2}}{\left[\dfrac{\ln 2}{\Delta\omega^2}\right]^2+2\alpha^2}, \quad (3)$$

and a stretched pulse duration τ

$$\tau^2=\tau_0^2+\left[\frac{8\alpha\ln 2}{\tau_0}\right]^2, \quad (4)$$

where the α is the chirping parameter and is determined by the experimental condition. If $\alpha\gg\tau_0^2$, the instantaneous frequency changes linearly in time during the pulse, with the rate of change $d\omega/dt$ being approximately inversely proportional to the chirping parameter α:

$$\omega(t)=\omega_0+\frac{\alpha\left[\dfrac{\Delta\omega^2}{\ln 2}\right]^2}{8+2\alpha^2\left[\dfrac{\Delta\omega^2}{\ln 2}\right]^2}t, \quad (5)$$

For the field linearly polarized along the z direction, the time-dependent Schrödinger equation is

$$i\hbar\frac{\partial}{\partial t}|\Psi\rangle=\left\{\frac{\hat{\mathbf{P}}^2}{2\mu}+\hat{V}_l(R)-\mathbf{E}(t)\cdot\hat{\boldsymbol{\mu}}(R)\right\}|\Psi\rangle, \quad (6)$$

where the effective potential $\hat{V}_l(R)=D_e[1-e^{-\alpha_M(R-R_o)}]^2+l(l+1)/(2\mu R^2)$ and $\mu(R)=(p_aR^2+p_bR+p_c)\exp[-p_d(R-p_e)^2]$, $p_a=0.2772$, $p_b=-0.6426$, $p_c=-4.9012\times10^{-7}$, $p_d=0.5363$, and $p_e=1.6462$, which is fitted by the *ab initio* calculation results [22]. The above time-dependent system is propagated by the split-operator algorithm [23]. The state function is expanded into partial waves:

$$\psi(R,\Omega;t)=\sum_{l=0}^{l_{max}}F_l(R;t)Y_{l,m}(\Omega). \quad (7)$$

The state function is transformed alternatively between coordinate and momentum space by the fast-Fourier transform method [24]. For the linearly polarized field, the magnetic quantum number m is conserved and hence the system is actually two dimensional. In addition, the propagation of the dipole coupling term can be analytically solved. Since

$$e^{\pm ik\mu(R)\cos\theta}=\sum_{n=0}^{\infty}(\mp i)^n\sqrt{4\pi(2n+1)}j_n(k\mu(R))Y_{n,0}(\Omega), \quad (8)$$

the following expansion can be made:

$$e^{\pm ik\mu(R)\cos\theta}\psi(R,\Omega;t)=\sum_{l=0}^{l_{max}}G_l(R;t)Y_{l,m}(\Omega). \quad (9)$$

Then, the time-dependent radial part becomes

$$\begin{aligned}G_{l'}(R;t)=&\sum_{n=|l-l'|}^{n=l+l'}\sum_{l=0}^{l_{max}}(-1)^m(\pm i)^n(2n+1)\\&\times\sqrt{(2l+1)(2l'+1)}j_n(k\mu(R))F_l(R;t)\\&\times(-1)^{2(l'-n)-m}(2l+1)^{-1/2}\langle l'0;n0|l0\rangle\\&\times\langle l'-m;n0|l-m\rangle, \quad (10)\end{aligned}$$

where $\langle l_1m_1l_2m_2|l_3m_3\rangle$ is the Clebsch-Gordan coefficient, $\Omega=(\theta,\phi)$, $k=|E(t+\Delta/2)|\Delta$ and $j_n(k\mu)$ is the spherical Bessel function of order n.

In the numerical calculation, corresponding experimental parameters are followed. The NO molecule is irradiated by the (sub)picosecond chirped pulse with intensity $I_{chirp}=E_m^2$. Assume that there is no energy loss before and after chirping, the output pulse has a field strength $E_m=\sqrt{I_{max}\tau_0/\tau}$, which is smaller than the input pulse field strength due to the stretched duration, and the input pulse intensity $I_{max}=10^{10}$ W/cm^2. The infrared laser frequency is 1850 cm^{-1} with a bandwidth limit 40 cm^{-1} [18]. In our calculation, 48 a.u. for a span of the radial coordinate, 2048 grid points, and 7–8 partial waves in angular expansion, are used. The population of the highest angular-momentum partial wave is less than 10^{-16} at the end of the pulse. In the field-free calibration, the norm of the wave function is accurate to the 11th decimal point during 0.37-ps propagation. This guarantees that our presentation of small probability is reliable.

The population probability of the νth state $P_\nu(t)$ is defined as

$$P_\nu(t)\equiv\sum_{l=0}^{l_{max}}P_{\nu,l}(t), \quad (11)$$

where $P_{\nu,l}(t)=|\langle\phi_{\nu,l}(t)|\psi(t)\rangle|^2$ denotes the population of the lth rotational level of the νth vibrational state at time t and $\nu=0,1,2,\ldots,54$.

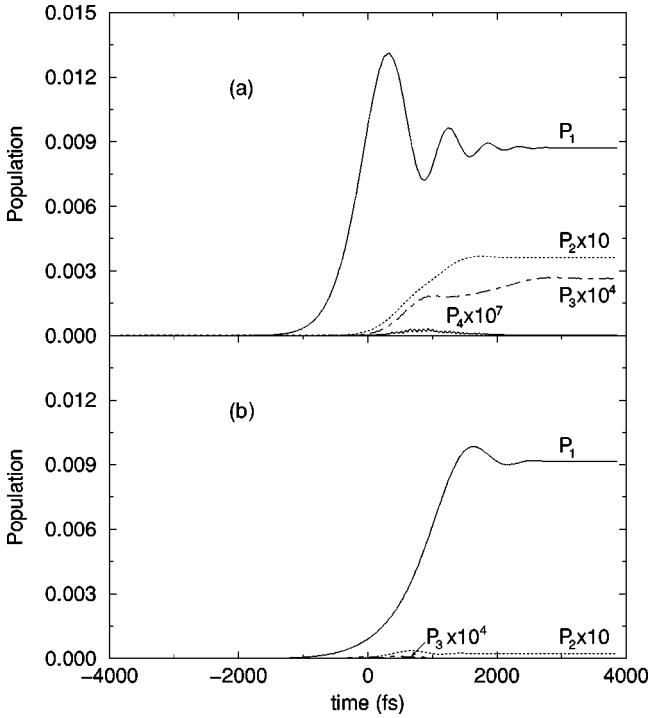

FIG. 1. Population history of some vibrational states P_ν under the linear chirped pulses: (a) $\alpha=-10^{-25}$ s^2, and (b) $\alpha=10^{-25}$ s^2. Note that the fifth state, $\nu=4$, is too small to be visible in (b) even after scaling by a factor of 10^7.

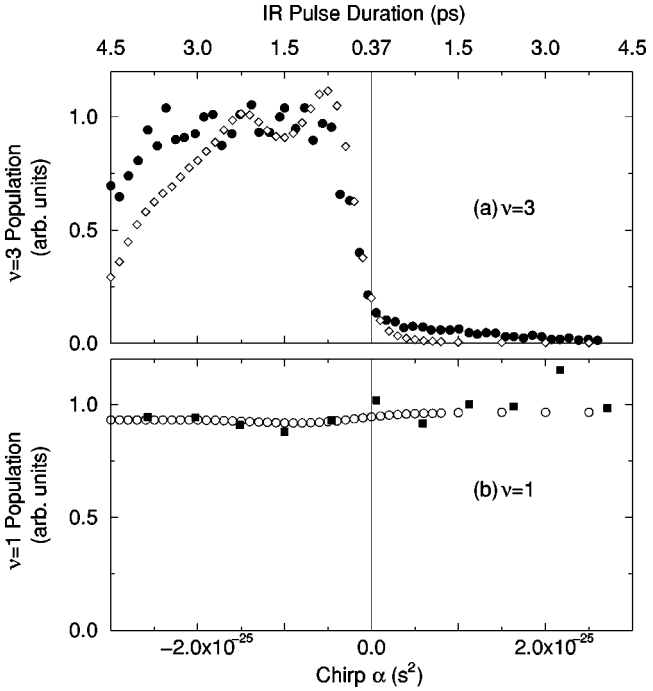

FIG. 2. Populations of vibrational states as a function of chirping parameter α. The stretched pulse duration due to the chirping are shown at the top axis. The numerical results are scaled to compare with the experimental data; see the text for details. (a) Vibrational state $\nu=3$ populations; filled circles are experimental data from Maas *et al.* [18] and and open diamonds are calculations of this work. (b) Vibrational state $\nu=1$ populations. The filled squares are Maas *et al.*'s data and the open circles are the results of our calculations.

III. RESULTS AND DISCUSSION

We first depict the populations of excited states vs time. Figure 1(a) is the result of negative chirping with $\alpha=-1.0\times10^{-25}$ s^2, and Fig. 1(b) is for $\alpha=1.0\times10^{-25}$ s^2. We can see from these results that the first excited-state population for negative chirping is always larger than the positive one during the interaction time, although the final populations are almost the same in both cases. This reflects the fact that the negative α case matches the blue-to-red change of the vibrational ladders. The positive α case tunes the frequency oppositely and is chirped in the ''wrong'' direction, as indicated in the experiments [17,18]. As shown in Fig. 1(a), we can see that part of the first excited-state population is pumped to upper levels sequentially, while most of the first excited-state population in the negative chirping case is dumped back into the ground state. This is due to the two-level excitation characteristics and the interference between a ''red'' P branch and a ''blue'' R branch [17,25]. The mechanism is that, when the $(\nu=0,\ l=0)$ initial state has been pumped into the state $(\nu=1,l=1)$, the intermediate state can be further pumped up into $\nu=2$, $l=0$ (the ''red'' P branch) or into $\nu=2$, $l=2$ (the ''blue'' R-branch); however, the former process is preferred due to the lower transition frequency while the field frequency is chirped into lower region. On the other hand, the intermediate state can also undergo stimulated emission to $\nu=0$, $l=0$ and $\nu=0$, $l=2$; again the latter one is preferred for the lower frequency for the same reason.

In Fig. 2, we compare our calculated results with the measurements of Maas *et al.* [18] for the initial state prepared in the vibrational ground state with zero rotational quantum number. The populations are normalized with respect to $\alpha=-1.5\times10^{-25}$ s^2 for $\nu=3$ in Fig. 2(a), and are normalized with respect to $\alpha=-5.0\times10^{-26}$ s^2 for $\nu=1$ in Fig. 2(b). From Fig. 2(a), the numerical results are in good agreement with the experimental data for most α values. The calculation shows minor deviations from the experimental results only at α smaller than -2.0×10^{-25} s^2. The deviations are mainly for the following reasons: (i) the pulse bandwidth is smaller than the experimental value, 50 cm^{-1}, and the transition frequency of neighboring states is slightly different from the experiment; (ii) the populations must be averaged over all the possible states in thermal equilibrium. The contribution from other thermal states must be taken into account when the temperature is not very low [18]. In Fig. 2(b), the first excited-state population is nearly equal and saturated against the chirps. This is because the chirped pulses always sweep across the resonance frequency between $\nu=0$ and $\nu=1$ ($\omega_0=1863$ cm^{-1}) around the maximum pulse intensity in both chirping directions during the interaction time.

Classically, the molecular systems that have a larger dipole moment along the field polarization direction will be more easily excited by the external field. Maas and coworkers [17,18] measured of the rotational excitations from the vibrational ground state with $l=0$ and $l=1$ into the first and third vibrational excited states. To investigate the angular effects on these excitations, Fig. 3(a) and 3(b) show the cases of chirped excitation from the initial states of the vibrational ground states with angular parts Y_{00} and Y_{10} in states of $\nu=1$ and 3, respectively. We find that the $\nu=3$

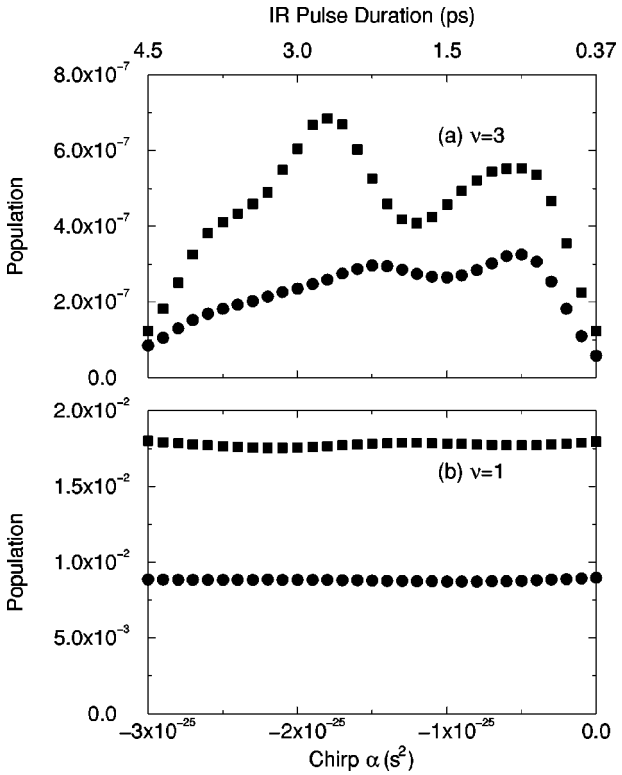

FIG. 3. Rotational populations of vibrational states vs α for different initial states: (a) $\nu=3$ populations; filled circles are initial state prepared at $\nu=0$ and $l=0$ with magnetic quantum $m=0$, while filled squares are for initial state $\nu=0$, $l=1$ and $m=0$; (b) same as (a) except the populations are for the $\nu=1$ vibrational state.

population of $l=1$, $m=0$ is clearly larger than the $l=0$ and $m=0$ case in Fig. 3(a). But the population difference of the two partial waves with respect to the chirping parameter α for $\nu=3$ is not as uniform as those of $\nu=1$ in Fig. 3(b). This implies that the Y_{10} spatial distribution has a larger probability along the field polarization direction and is more easily excited to higher states than Y_{00}. Again, the $\nu=1$ population reveals saturation of excitation against the chirping in Fig. 3(b).

Although the calculation results are in good agreement with the experimental data, it is worthwhile to investigate the poor population transfer in the chirping excitation. We plot the time dependence of the instantaneous frequency $\omega(t)$ and the pulse amplitude $E_m \exp(-\Gamma t^2)$ in Fig. 4. As we can see in Fig. 4, the pulse amplitude is smaller and broader when the chirping parameter value ($|\alpha|$) increases. On the other hand, the frequency sweep (chirping rate) becomes more and more slow to match the weaker adiabatic condition as the chirping parameter increases. The two factors compete and determine the excitation efficiency. As a result, the fast chirping rate (small α) and low pulse amplitude (large α) have a smaller excitation population of high vibrational states. Figure 4 also shows that the $\nu=0\rightarrow\nu=1$ and $\nu=1\rightarrow\nu=2$ transitions do not take place in the maximum region of the pulse amplitude, which is another factor resulting in the poor excitation population. In Fig. 5(a) we calculate the populations of $\nu=1$ and $\nu=3$ states by varying the central frequency ω_0 from 1800 cm^{-1} to 1900 cm^{-1} at $\alpha=1.5\times10^{-25}$ s^2 and $\tau_0=370$ fs and by changing the duration at $\alpha=1.5\times10^{-25}$ and $\omega_0=1850$ cm^{-1} in Fig. 5(b). In Fig.

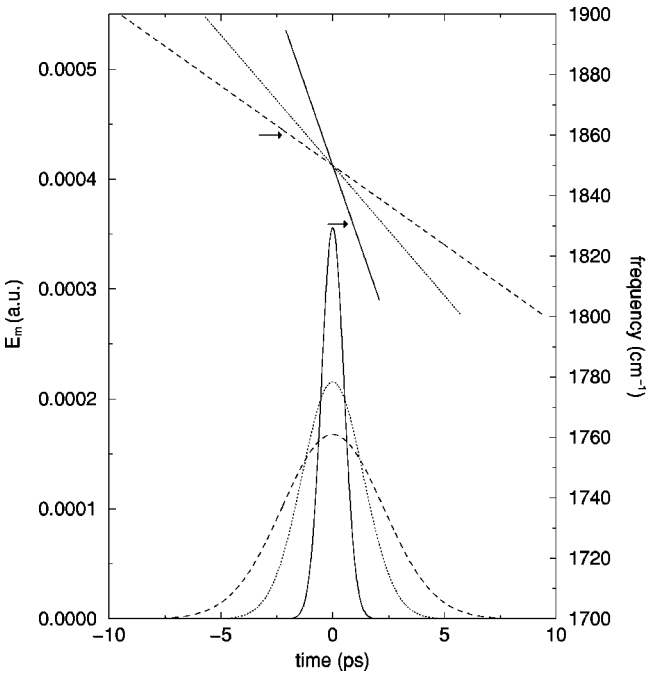

FIG. 4. Time dependence of pulse amplitude $E_m \exp(-\Gamma t^2)$ and frequency $\omega(t)$. Solid line; $\alpha=5\times10^{-26}$ s^2; dotted lines: $\alpha=1.5\times10^{-25}$ s^2; and dashed lines, $\alpha=2.5\times10^{-25}$ s^2. The arrows indicate the $\nu=0$, $l=0\rightarrow\nu=1$, $l=1$ transition at 1863 cm^{-1} and $\nu=1$, $l=1\rightarrow\nu=2$, $l=2$ transition at 1829 cm^{-1}.

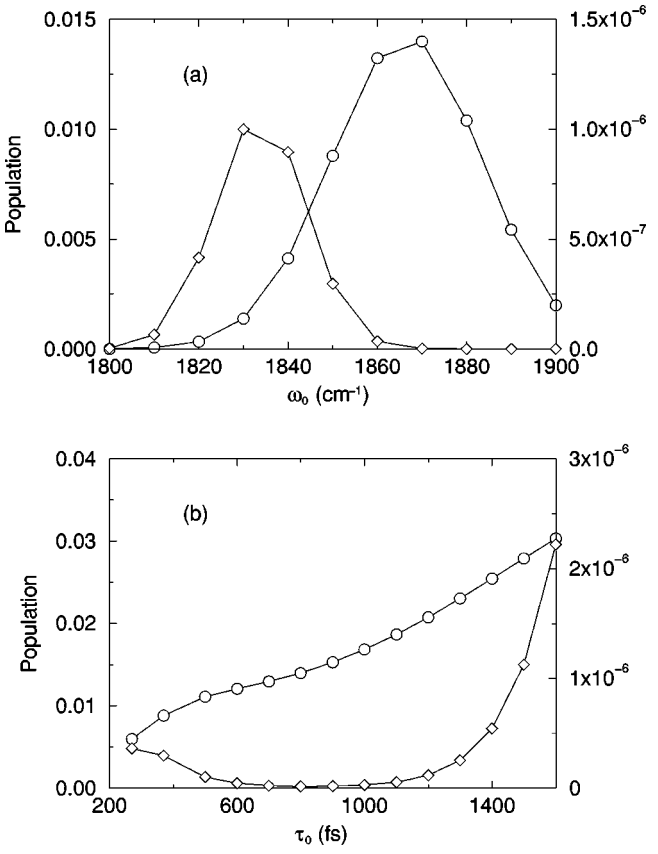

FIG. 5. P_1 (circles, left scale) and P_3 (diamonds, right scale) populations vs central frequency ω_0 and pulse duration τ_0. (a) $\alpha=1.5\times10^{-25}$, $\tau_0=370$ fs, and $I_{max}=10^{10}$ W/cm^2. (b) $\alpha=1.5\times10^{-25}$, $\omega_0=1850$ cm^{-1}, and $I_{max}=10^{10}$ W/cm^2.

TABLE I. The chirping rate $d\omega/dt$, pulse duration τ, and peak field strength E_m for three chirping parameters with input pulse intensity 10^{10} W/cm^2 and duration $\tau_0=370$ fs. Only the transition moments, $d_{\nu' l',\nu l}\equiv\langle \nu' l'|\hat{\boldsymbol{\mu}}(R)\cdot\mathbf{e}_z|\nu l\rangle$, between $\nu'=\nu+1$ and $l'=l+1$ are shown.

α (s^2)	$d\omega/dt$ (a.u.$^{-2}$)	τ (fs)	E_m (a.u.)	$d_{\nu' l',\nu l}$ (a.u.)
10^{-26}	4.18×10^{-9}	399.2	5.14×10^{-4}	$d_{00,11}=1.97\times10^{-2}$
1.5×10^{-25}	1.90×10^{-9}	2278.3	2.15×10^{-4}	$d_{11,22}=2.47\times10^{-2}$
2.5×10^{-25}	1.16×10^{-9}	3765.0	1.67×10^{-4}	$d_{22,33}=2.95\times10^{-2}$

5(a) the central frequency will determine the time of the consecutive transitions. There is no significant population increase around $\omega_0=1850$ cm^{-1}. As the τ_0 increases, the stretch of the chirped pulse is small and the large and long pulse amplitude makes it match the adiabatic condition better than the short duration. The increase of populations is still not so prominent. A careful check of the adiabatic condition for this chirped pulse and NO system will elucidate the inefficient excitation. Table I lists the chirping rate $d\omega(t)/dt$, field strength E_m, and transition moment $d_{\nu' l',\nu l}\equiv\langle \nu' l'|\hat{\boldsymbol{\mu}}(R)\cdot\mathbf{e}_z|\nu l\rangle$ for three chirping parameters. From

$$\Omega_{Rabi}(t)=d_{\nu' l',\nu l}E_m\ \exp(-\Gamma t^2), \tag{12}$$

where ν' and ν are two neighboring states and $l'=l\pm1$, the weaker adiabatic condition $|d\omega(t)/dt|\ll\Omega^2_{Rabi}(t)$ is not satisfied in the NO case due to the low intensity, and the chirping excitation is inefficient. Slowing down the chirping rate also stretches the pulse duration and as a result decreases the output laser intensity if the energy is conserved before and after the chirping. Therefore, having significant excitation within picoseconds, one has to increase the pulse intensity or the chirping parameter of longer pulse duration.

IV. CONCLUSIONS

In summary, we have given the calculated results, including the rotational degree of freedom in the calculation of chirping excitation, and compared them with the experimental results. To our knowledge, this is the first comparison between theory and experiment of the chirped pulse excitation of the NO molecule. Experimental data show a rotational temperature of $T=15$ K for $\nu=0$. The effect of the free-electron laser on the vibrational transitions is two orders of magnitude larger than the thermal effect. So the neglect of the thermal effect in this paper is reasonable for higher vibrational excited states. For a future investigation, thermal distribution will be considered for other higher l initial states, and the interference between states will be explored.

ACKNOWLEDGMENTS

The authors acknowledge the National Science Council of Taiwan for financial support under Contract Nos. NSC88-2811-001-0050 and NSC88-2112-M009-009. T.F.J. thanks Professor L.D. Noordam and Dr. D.J. Maas for their papers on the experiments with NO.

[1] M. Kaluža, J. T. Muckerman, P. Gross, and H. Rabtiz, J. Chem. Phys. **100**, 4211 (1994).
[2] S. Chelkowski, A. D. Bandrauk, and P. B. Corkum, Phys. Rev. Lett. **65**, 2355 (1990).
[3] S. Chelkowski and A. D. Bandrauk, Phys. Rev. A **41**, 6480 (1990); Chem. Phys. Lett. **186**, 264 (1991); J. Chem. Phys. **99**, 4297 (1993).
[4] B. Just, J. Manz, and I. Trisca, Chem. Phys. Lett. **193**, 423 (1992); B. Just, J. Manz, and G. K. Paramonov, *ibid.*, **193**, 429 (1992).
[5] J. S. Melinger, D. McMorrow, C. Hillegas, and W. S. Warren, Phys. Rev. A **51**, 3366 (1995).
[6] S. Guérin, Phys. Rev. A **56**, 1458 (1997).
[7] W. K. Liu, B. Wu, and J. M. Yuan, Phys. Rev. Lett. **75**, 1292 (1995).
[8] J. M. Yuan and W. K. Liu, Phys. Rev. A **57**, 1992 (1998).
[9] C. E. Hamilton, J. L. Kinsey, and R. W. Field, Annu. Rev. Phys. Chem. **37**, 493 (1986).
[10] M. Drabbels, A. M. Wodtke, M. Yang, and M. H. Alexander, J. Phys. Chem. A **101**, 6463 (1997).
[11] S. Schiemann, A. Kuhn, S. Steuerwald, and K. Bergmann, Phys. Rev. Lett. **71**, 3637 (1993).
[12] G. van den Hoek, M. Jonker, D. H. Parker, C. A. Taatjes, and S. Stolte, Chem. Phys. Lett. **215**, 461 (1993).
[13] K. K. Lehmann, G. Scoles, and B. H. Pate, Annu. Rev. Phys. Chem. **45**, 241 (1994).
[14] J. Allen and J. H. Eberly, *Optical Resonance and Two-Level Atoms* (Wiley, New York, 1975).
[15] J. T. Lin, T. L. Lai, D. S. Chuu, and T. F. Jiang, J. Phys. B **31**, L117 (1998).
[16] J. T. Lin, D. S. Chuu, and T. F. Jiang, Phys. Rev. A **58**, 2337 (1998).
[17] P. Balling, D. J. Maas, and L. D. Noordam, Phys. Rev. A **50**, 4276 (1994).
[18] D. J. Maas, D. I. Duncan, R. B. Vrijen, W. J. van der Zande, and L. D. Noordam, Chem. Phys. Lett. **290**, 75 (1998).
[19] T. Seideman, J. Chem. Phys. **103**, 7887 (1995).
[20] M. V. Korolkov, G. K. Paramonov, and B. Schmidt, J. Chem. Phys. **105**, 1862 (1996).
[21] E. B. Treacy, IEEE J. Quantum Electron. **5**, 454 (1969).
[22] F. P. Billingsley II, J. Chem. Phys. **62**, 864 (1975).
[23] M. D. Feit, J. A. Fleck, Jr., and A. Steiger, J. Comput. Phys. **47**, 412 (1982).
[24] M. D. Feit and J. A. Fleck, Jr., J. Chem. Phys. **78**, 2578 (1984).
[25] J. S. Melinger, S. R. Gandhi, A. Hariharan, D. Goswami, and W. S. Warren, J. Chem. Phys. **101**, 6439 (1994).